Published as:
Simmons SC, Dellinger G, Mendes C, Lubitz WD. Development of a Computational Fluid Dynamics Model for Archimedes Screw Pumps. Responsible Engineering and Living. Springer Nature. 2023. ISBN 978-3-031-20505-7

Development of a Computational Fluid Dynamics Model for Archimedes Screw Pumps

Scott C. Simmons[1,3][0000-0002-6558-9632], Guilhem Dellinger[2][0000-0002-5537-8225], Catarina Esposito Mendes[1], and William David Lubitz[1][0000-0003-3862-2895]

[1] School of Engineering, University of Guelph, Guelph ON N1G 2W1, Canada
[2] École nationale du génie de l'eau et de l'environnement de Strasbourg (ENGEES), Strasbourg 67000, France
[3] ssimmons@uoguelph.ca

Abstract. Archimedes screw pumps (ASPs) have been used for land drainage, irrigation, and conveyance of mixed media for millennia. Due to their simple, robust design, modern ASPs are commonly used for land drainage and reclamation, as well as flood management and wastewater conveyance. In a climate-impacted future, the development of improved water management technologies is integral; however, design methods for ASPs are not well documented in the published literature. The design of screw pumps seems largely empirical. The leading text in screw pump design was compiled by Nagel in 1968, which predominantly sourced models and material from a Dutch paper by Muysken in 1932. The text uses many simplifications and empirical models based off undocumented experiments. So, there is a need to introduce more data and design insight to the literature to evaluate previous models, and develop more in-depth models to predict screw pump performance more accurately. Gathering data from operating screw pumps can be difficult, particularly since characterizing a wide range of operating conditions and screw geometries is desired for modelling purposes; both are conditions that cannot be easily changed in an operating pumping station. So, a Computational Fluid Dynamic (CFD) model was developed to allow for simulation of any screw geometry or operating configuration. The model used OpenFOAM 8 to simulate the two-phase, immiscible flow of water and air through a dynamically-mesh, full-scale Archimedes screw pump. A mesh-sensitivity study, and an evaluation study that compared simulated data to previously collected laboratory experiments, demonstrated that the simulation was an accurate approximation of screw pump performance. Once the model was deemed appropriate, it was used to collect data across a wide range of operating conditions and two scale-sized screw pumps.

Keywords: Archimedes Screw Pump, Land Drainage, Wastewater, Computational Fluid Dynamics, Pumping, Hydrodynamic Screw, Land Reclamation.

1 Introduction

Archimedes screws (also termed hydrodynamic screws or Egyptian screws) have been used for a variety of applications for nearly three thousand years; however, their modern

design is not well documented in the literature. Screw pumps are often used for land reclamation, drainage, and wastewater management; in a climate-impacted future, their use will be integral. As such, there is a need to investigate the performance of existing screw installations and introduce high-quality performance data to the literature to evaluate and improve the accuracy of design guidelines. An Archimedes screw is a helical array of one or more blades wrapped around a central, cylindrical tube. It is often used as a hydraulic machine to pump water; in this configuration it is called an Archimedes screw pump (or screw pump). To perform pumping action, the screw is turned within an inclined trough or tube. The end of the screw is partially submerged in water such that, as it turns, it encloses water between its blades. The enclosed volume of water is often called a "bucket" of water [1].

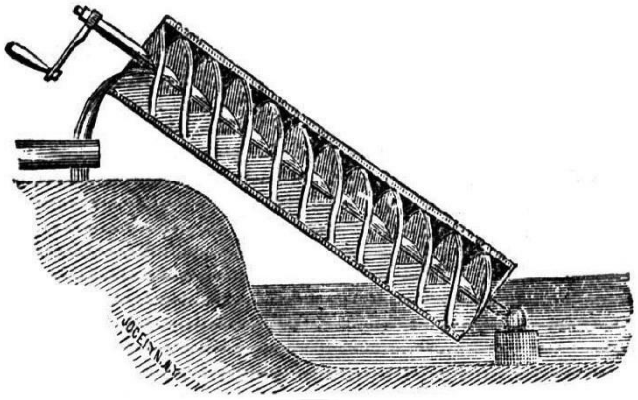

Fig. 1. drawing of a hand-crank Archimedes screw pump [1].

1.1 Background

The Archimedes screw found use in the 7th century BCE Neo-Assyrian Empire of Sennacherib (704-681 BCE) where it was employed as an irrigation device [2]. It was commonly used for irrigation and other pumping applications in antiquity. The famous Greek philosopher, mathematician, physicist, and astronomer, Archimedes of Syracuse popularized use of the device for irrigation in Egypt's Nile Delta (circa 287 BCE) [1], and as the first documented bilge pump on a Syracusan naval flagship [3].

The Archimedes screw has been used for drainage of the Roman Empire's mines in the Iberian peninsula (1st century BCE to 5th century CE) [4], irrigation in the territories of the Abbasid Caliphate [circa 1100 CE] [5], for land reclamation in the Netherlands (from circa 1600 CE – present) [6], for drainage in Japan (1637 CE) [7], for ship propulsion in Europe (1839 CE) [8], and as a hydroelectric generator (1990s – present) [9]. As a hydroelectric energy conversion device, it is often called an Archimedes screw generator.

In the modern day, it is common to see Archimedes screws used for water [10] and wastewater pumping [11], as a conveyor for grains and granular solids [12], [13], a fish ladder [14]–[16], a drive mechanism for amphibious vehicles [17], and injector for

plastic molding [18], for heart valve replacements [19], land reclamation [6], and hydropower generation [20].

There has been little advancement in the literature on Archimedes screw pumps in the last few decades. Monserrat et al. (2015) published an investigation of cost-saving techniques for screw pump design; it explored the use of a variable inclination-angle screw pump [21]. The only other recent English-language contribution was an experimental investigation of a laboratory-scale screw pump's performance to address the lack of literature and data, and to examine parallels between ASPs and ASGs [22].

Based on the literature and historical context, the modern design of the ASP had primarily evolved in a region that is now within the Netherlands. During the Dutch Golden Age (late 1500s to late 1600s), ASPs were used to drain the marshes and fenlands in the Netherlands [23], [24]. The artificially drained regions of the Netherlands are called polders, and historically, the Dutch have used polder mills to maintain reclaimed lands. Polder mills are traditional Dutch windmills that power water pumps – it was very common for polder mills to utilize screw pumps since they could move large volumes of water across a low head effectively [8]. Early ASP polder mills could pump water to a head of roughly 1.5 meters. As the technology developed, and designs improved, higher heads were achievable. Modern steel screw pumps can bridge heights of 4 to 5 meters [6]. In the 1930s CE, there were approximately 300 screw pumps used for lowland drainage and flood control in the Netherlands alone; most of those pumps were still wind-powered [8]. Due to its widespread use, many leading manufacturers of modern screw pumps are based in the Netherlands, or low-lying regions nearby.

Since the technology has been in use globally since antiquity, it is very difficult to find design guidance in the literature; the technology seems to have developed by experience. Most published screw pump literature documents empirically derived design guidance [3].

Nagel's Screw Pump Handbook [25] seems to be the most complete design manual in the published English-language literature. Nagel's handbook was revised in a 1988 German-language publication [8] – an English translation of the revision does not seem to exist in the available literature. Nagel draws from a small variety of Dutch- [26], [27] and German-language [28]–[31] publications, as well as his own design experience in the handbook. Aside from Nagel's work in 1959 [30], all models presented in Nagel's handbook seem to be developed between 1851 and 1932; though some citations were not dated.

Muysken's publication [26] seems to be the most referenced in Nagel's Handbook; Muysken's work is itself a comprehensive collection of design models and guidelines by the author, and from earlier Dutch- and German-language publications. It is noted that, generally, that means the state-of-the-art design guidance for Archimedes screw pumps was published nearly 100 years ago (at time of publication). There have been substantial technological and computational developments since that time. Additionally, it is often difficult to find publications relating to the experiments and data used to derive the empirical relationships presented in the literature.

So, the goal of this study is to document the design, evaluation, and implementation of a novel computational fluid dynamic (CFD) model of an Archimedes screw pump (ASP). Using modern technology and computational techniques, a CFD model was

developed that characterized an accurate approximation of screw pump performance. The model was evaluated against experimental data and used to conduct a preliminary investigation into screw pump performance to introduce more comprehensive data to the literature for future numerical model developments. Future model developments, like the development of a first-principles numerical performance model, are integral to develop more accurate screw pump design optimization guidelines.

1.2 Screw pump design and terminology

A diagram of the dimensions and variables used to describe Archimedes screw pumps is shown in Fig. 2.

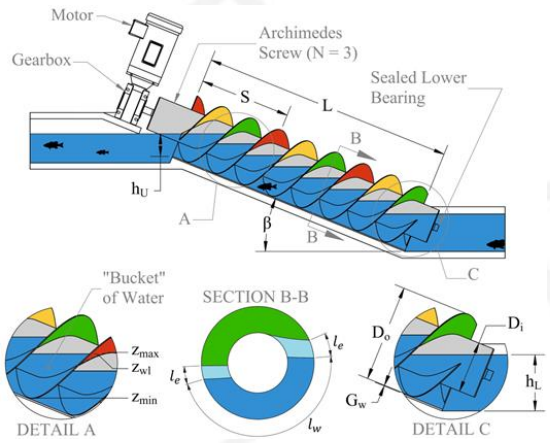

Fig. 2. Archimedes screw pump dimensions and variables.

Archimedes screws are mostly described geometrically by their outer diameter (D_o) and length (L). Practically, designers and users usually refer to a screw by its designed flow rate (Q), and head (h). However, a more robust set of dimensions is required to model and describe these parameters in detail. To fully describe the functional geometry of a screw, a designer uses the outer diameter, inner diameter (D_i), screw pitch (S), screw length (L), the number of blades (N), the gap width (G_w), and the inclination angle of the screw (β).

The screw is also often described in terms of its operating parameters, such as the upper water level (h_U), lower water level (h_L), and rotation speed (ω). These parameters are the main input parameters during operation, they drive the flow rate and power requirements of the screw.

The mechanical power required to rotate the screw (P_s) is a function of the torque (T) and rotation speed requirements of the screw during operation. The torque is largely due to the static pressure of the water in the screw's buckets during conveyance. Therefore, in mathematical modelling, the fill height of the screw's buckets (z_{wl}) is a very important parameter; it is most used as a dimensionless bucket fill height ratio (f). The

bucket fill height ratio is a function of the fill height of the bucket and the minimum (z_{min}) and maximum (z_{max}) height limits within the bucket.

$$f = \frac{z_{wl} - z_{min}}{z_{max} - z_{min}} \tag{1}$$

When the bucket fill height ratio is $f = 1$, the buckets are perfectly full. If the fill height is $f > 1$, the buckets experience overflow; water spills over the top of the central cylinder and into the next bucket between the same blades (one pitch-length down the screw). If the fill height ratio is $f < 1$, the screw is underfilled and will not undergo overflow leakage. Generally, it is desired to keep the bucket fill height ratio as close to $f = 1$ as possible. This guideline maximizes the volume of water transported and minimizes overflow leakage; however, it is a general practice that has not been proven to be physically optimal.

To achieve the desired fill height ratio, designers must install the screw at a height corresponding to the optimal lower water level. Alternatively, control structures may be used to manipulate intake water levels. In either case, the optimal lower water level (h'_L) of the screw corresponds to the height of water of the first fully enclosed bucket at the lower end of the screw. Usually, the upper and lower water levels of the screw are described in dimensionless terms. These variables are called the upper (ψ_U) and lower (ψ_L) submergence levels; since they are effectively the ratio of the amount the screw ends are submerged in water.

$$\psi_U = \frac{h_U}{D_o \cos\beta} \tag{2a}$$

$$\psi_L = \frac{h_L}{D_o \cos\beta} \tag{2b}$$

A submergence level of $\psi_L = 1$ would indicate that the lower end of the screw is 100% submerged under water. Screw pumps usually require lower submergence levels between 60% to 80% to operate optimally. The optimal lower submergence of a specific screw may be calculated as follows [32]:

$$\psi'_L = \frac{D_i + D_o}{2D_o}\sqrt{1 - \left(\frac{S\tan\beta}{\pi D_i}\right)^2} \tag{3}$$

To operate with the most mechanical efficiency, it is postulated that the upper submergence of the screw should be set to an optimal height that is non-zero. The optimal height should correspond to a height in which the upper water level supplies a back-pressure to the screw's buckets while they empty. Theoretically, this would prevent premature leakage and allow water to exit the screw in a more beneficial flow regime. However, in practice, screw pump designers usually set the upper submergence level to $\psi_U \leq 1$. Using this submergence guideline allows designers to forego the use of back-flow valves and other flow control structures to prevent back-flow through the screw when it is not operating.

The most common design of Archimedes screw pumps has the screw rotating in a fixed trough. To prevent premature wearing of the screw's blades, there is a small, designed gap between the blade tips and the trough. The screw's blade-trough gap is usually described by its width (G_w); screw gap widths are usually between G_w = 2 to 12 mm depending on the size of the screw. Nagel suggests an empirical relationship to design the gap width of an installation:

$$G_w = 0.0045\sqrt{D_o} \tag{4}$$

The screw's trough is usually either made of formed steel or is concrete and cast-in-place. Some alternative designs of Archimedes screw pumps affix the tough to the screw's blade tips and rotate the entire assembly to achieve a desired flow and head. Though the gap is eliminated in this configuration, other losses are introduced to the system.

In conventional, fixed-trough screw pump designs, the gap is essential to extend the operating life of the installation; however, the gap introduces a form of loss due to a leakage flow. The gap width is large enough to prevent wearing in the screw but minimized to mitigate the effects of the gap leakage (Q_g) flow rate. Therefore, in a well-designed screw installation, the gap leakage is proportionally small when compared to the overall system flow. Muysken [26] defined the gap leakage as follows:

$$Q_g = l_1 \mu G_w D_o \sqrt{D_o} \tag{5}$$

Where μ is an effluent coefficient and l_1 is a shape factor that is a function of the inner diameter, outer diameter, pitch, and inclination angle. Muysken [26] also presented a less accurate, but simplified version of the relationship which was later presented in Nagel's screw pump handbook.

$$Q_g = 2.5\ G_w D_o \sqrt{D_o} \tag{6}$$

The total flow rate that a screw pump can deliver at its top was described by Muysken as a function of rotation speed (in rev/min), outer diameter, and a geometric flow factor (q) that can be found through integration, or in look-up tables. Values for the flow factor may be found in Muysken's publication [26], the screw pump handbook [8], [25], or a more recent review of screw pump design guidelines [33]. Muysken found that flow rates usually exceeded estimated values by 10% to 12% and in some cases up to 30%, so the calculation was scaled by 1.15 to bring it more in line with real-world measurements.

$$Q = 1.15 \cdot q\omega D_o^3 \tag{7}$$

Nagel suggested that the flow rate relationship could be further simplified to eliminate the rotation speed term, if designers used the recommended rotation speed for the screw. Muysken presented four models for rotation speed, and recommended an improvement; Nagel suggests that Muysken's recommendation was the most practical. The improved model was as follows, where rotation speed is in revolutions per minute:

$$\omega = \frac{50}{\sqrt[3]{D_o^2}} \tag{8}$$

Using this relationship, Nagel suggested the flow rate could be presented independent of rotation speed as follows:

$$Q = 57.5 \cdot qD_o^2\sqrt[3]{D_o} \tag{9}$$

The transport velocity is another important variable in mathematical modelling of screw pumps. The transport velocity describes the linear conveyance of the screw's buckets during operation. As such, it is a function of the screw pitch and rotation speed (in rev/min).

$$v_T = \frac{S\omega}{60} \tag{10}$$

A screw pump installation is usually designed for a desired flow rate and height requirement. As such, flow rate is usually a known input to a designer. Muysken suggests that the flow rate equation should be rearranged to solve for the outer diameter requirement. It was noted that the corrective term of 1.15 should be removed from the relationship so the screw's size allows it to supply more than its rated delivery flow rate if required [25], [26]. The relationship was presented as follows, where omega is in units of revolutions per minute:

$$D_o = \sqrt[3]{\frac{Q}{q\omega}} \tag{11}$$

Screw pump geometries are often described by three dimensionless parameters, the: diameter ratio ($\delta = D_i/D_o$), pitch ratio ($\sigma = S/D_o$), and length ratio ($\lambda = L/s$). It was shown by Rorres [1] that the theoretical optimal diameter ratio is $\delta = 0.54$. Therefore, the inner diameter should be $D_i = 0.54 \cdot D_o$. In practice, the inner diameter is usually made up of a standard sized, round structural tubing, so designers should select the nearest standard size diameter.

It has been suggested that the pitch ratio should be set to $\sigma = 1$ (that the pitch should equal the outer diameter). This value was determined using a heuristic model and helps prevent additional costs of manufacturing [25]. Recent experimentation with Archimedes screw generators (the hydropower configuration) suggest that this guideline is reasonable [34].

Finally, the screw length is usually described in terms of the length ratio. The length ratio effectively describes how many pitch lengths the screw is; in other words, it describes how many revolutions each helical blade has. It is common to see screws with length ratios of above 1.5 or 2 – sometimes much higher at wastewater treatment facilities. Along with the inclination angle, the length of the screw dictates the height that water can be conveyed. Generally, a shorter-length screw will be less expensive since it has a smaller footprint and is made up of less material. However, to accomplish the same conveyed height, a shorter screw must be installed as a steeper inclination angle. This concept is easier to visualize in reference to the geometric head (h_g) relationship:

$$h_g = L \sin \beta \tag{12}$$

The geometric head is effectively the height of the screw from center-to-center. If the screw is designed shorter, the inclination angle must increase to make up the head difference. Both Muysken and Nagel suggest application-specific inclination angles for screw pumps. Muysken found that screws conveying water with an inclination angle of $\beta = 26°$ performed with a high mechanical efficiency. He suggested this is the most desirable inclination angle for dewatering and land reclamation installations with low delivery head requirements. Nagel and Radlik [8] suggest that some sites with higher height requirements could reasonably be installed at steeper inclination angles to save material costs at the expense of inefficiencies; it was noted that there was roughly a 3% drop in mechanical efficiency for every 1 degree increase in inclination angle. It was also noted that steeper inclination angles had substantially less loss in applications with suspended solids (i.e., wastewater, etc.) since there was less gap leakage flow rate.

The power required to operate a screw pump (often called the "shaft power", P_s) is an important parameter for determining an optimal screw pump design. The shaft power is largely a function of the static pressure of water in the screw's buckets. The torque of the screw's motor is used converted into conveyance by the screw pump. The power required to perform this action is effectively a function of the hydrostatic pressure in the buckets resolved about the screw's axis of rotation. The net power required to operate the screw also accounts for the power losses in the system; one of the most substantial power losses is due to friction of water on the screw blades during rotation. The sum of the frictional power loss ($P_{L,f}$) and the power required to raise the buckets is equal to the screw's shaft power.

Hydraulic power is the term used to describe the rate of useful work performed by the screw. If is calculated as follows:

$$P_w = \rho g h Q \tag{13}$$

The hydraulic power term is used to define the mechanical efficiency of a screw pump. The mechanical efficiency can be calculated as follows:

$$\eta = \frac{P_w}{P_s} \tag{14}$$

Larger screws tend to operate at higher mechanical efficiencies than smaller screws due to effects of scale on various components of power. For example, frictional power loss scales with the surface area of the screw (second order of length scale), while torque scales with the hydrostatic pressure of the buckets, which is volume dependent (third order of length scale). Screw pump efficiencies range from about 65% (small diameter screws) to 75% (large diameter screws [35]. It is suggested that with careful design and site-specific optimization, screw pumps may operate at up to approximately 85% including electrical system losses; this value was based on precedent observed in recent research into screw generator (hydropower configuration) operation [36]–[38]. The wide range in efficiency estimates was mostly due to a lack of documentation and data of screw pump performance. Due to the limited literature on screw pump design, it is very likely that many screw pumps are not designed at their mechanically optimum configuration. Additionally, it may be desirable to install a less efficient screw to minimize upfront project costs. There are many unknowns in screw pump design based on the current available literature.

2 Methods

This study introduces a novel computational fluid dynamic (CFD) model for Archimedes screw pumps to the literature. A sensitivity analysis was conducted to determine an appropriate mesh design. The CFD model was then evaluated against experimental data collected in the University of Guelph's Archimedes screw laboratory to determine model accuracy. Our research team had difficulty gaining access to data for full-scale screw pumps but had previously developed a similar model for Archimedes screw generators [34]; the ASG model was robustly validated against laboratory- and real-world scale screw generator data. Since similar design techniques were employed during development of this screw pump model, it is suggested that the model has a similar accuracy for large-scale screw pump performance as the previous model had for large-scale generators.

Once the model was deemed an accurate approximation of Archimedes screw pump performance, it was used to perform an analysis into screw pump performance across two scale-sizes of a proportionally identical screw.

2.1 Computational fluid dynamic model design

The free surface flow in an Archimedes screw pump is geometrically complex, unsteady, and mostly turbulent. To best approximate this flow, the incompressible Reynolds-averaged Navier-Stokes (RANS) equations were solved with Menter's Shear Stress Transport turbulence closure (k-ω SST) [39].

In the model, flow is governed by the continuity equation and the RANS equations with a Boussinesq eddy viscosity assumption. These models were solved with the open-

source CFD software OpenFOAM (version 8, The OpenFOAM Foundation, 2020). An Euler scheme was used for time discretization, second order central schemes were used for gradient and Laplacian discretization, and the divergence of velocity was discretized using a second order upwind scheme.

OpenFOAM's *interFoam* solver was used for the simulations; the solver models two-phase, incompressible, immiscible flow using the PIMPLE and volume of fluid (VOF) methods. The PIMPLE Algorithm is a combination of the PISO (Pressure Implicit with Splitting of Operator) and SIMPLE (Semi-Implicit Method for Pressure-Linked Equations) algorithms. The SIMPLE algorithm is used for steady-state cases, while the PISO method is used for transient cases. In effect, the PIMPLE algorithm makes use of the SIMPLE algorithm to solve for a "steady-state" condition at each time step of a transient simulation. An adaptive time step was used for the simulations; the algorithm iterates at each time step until it reaches an appropriate condition (i.e., Courant–Friedrichs–Lewy number, $Co \leq 1$).

As mentioned, to close the RANS equation system, the eddy viscosity was computed with the two-equation Menter's Shear Stress Transport model (k-ω SST). The model evaluates the y+ at wall boundaries, and a blending function to switch between the k-ε and k-ω models. Care was taken during design to ensure that the value of y^+ was either less than 2 or more than 30 to ensure the most accurate implementation of the k-ω or k-ε models, respectively.

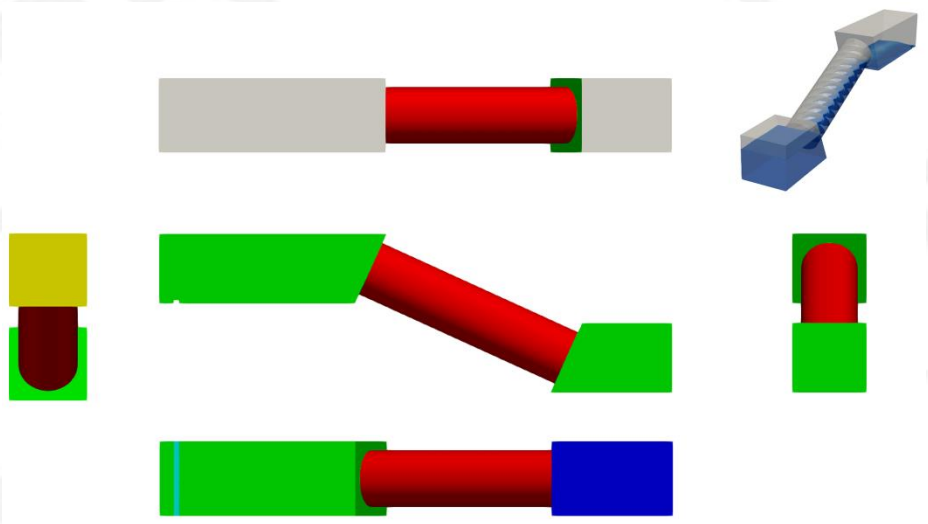

Fig. 3. simulation domain with boundaries coloured; trough (red), atmosphere (white), walls (green), inlet (blue), and outlet (yellow) are highlighted.

The screw domain (cf. Fig. 3) was designed such that the water inlet upwelled to mitigate the introduction of secondary flows. The inlet was set with a pressure-based boundary condition that allowed for control of water height. A dynamic mesh was used with arbitrary mesh interfaces (AMIs) to model the screw within the trough. For modelling

purposes, the screw was fully enclosed in the trough, though in practice, the trough is usually open topped. Each basin's top boundary was set to atmospheric conditions to prevent any pressure build-up in the air-phase of the fluid interaction. A fixed weir was set into the geometry of the upper basin to control the upper water level of the screw. Water passed over the weir and exited through the outlet; the outlet boundary was also set to atmospheric conditions to remove any impediments to discharge.

2.2 Sensitivity Study

The CFD model was designed with 5 different mesh refinement levels to perform a mesh sensitivity study.

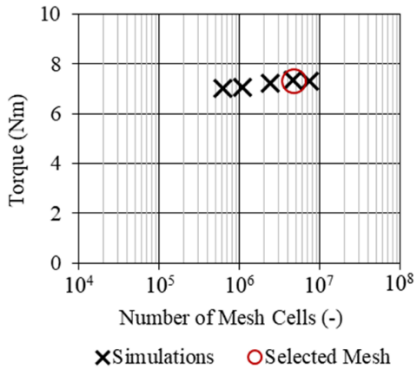

Fig. 4. mesh sensitivity analysis - selected mesh is highlighted.

It was found that the screw torque did not change substantially across the range of refinement levels, however it was least sensitive to change between refinement levels 4 and 5. As such, refinement level 4 was selected for the model since it yielded similar values to refinement level 5 but was computationally more efficient. The selected mesh had about 7.36 million cells.

2.3 Model Evaluation

The CFD model was compared to data previously gathered by the researchers in a set of laboratory experiments [22]. Three characteristic data points were simulated for comparison to the laboratory data. They had the following input parameters:

Table 1. experimental data points used for model evaluation - data is from a previous experimental study *[22]*

	D_o (m)	D_i (m)	S (m)	L (m)	N (-)	β (°)	ω (rev/min)	ψ_U (-)	ψ_L (-)
Run 1	0.316	0.168	0.318	1.219	3	26.4	73.6	0.00	0.39
Run 2	0.316	0.168	0.318	1.219	3	26.3	55.0	0.17	0.59
Run 3	0.316	0.168	0.318	1.219	3	26.3	36.5	0.45	0.78

There was a high degree of uncertainty in the laboratory experiments due to sensor accuracy and power loss in the screw's bearings; however, great care was taken to gather data as near to nominal measurements as possible. The experimental data was plotted directly against the simulated results in Fig. 5. The dotted line represents the when the experimental power is equal to the simulated power.

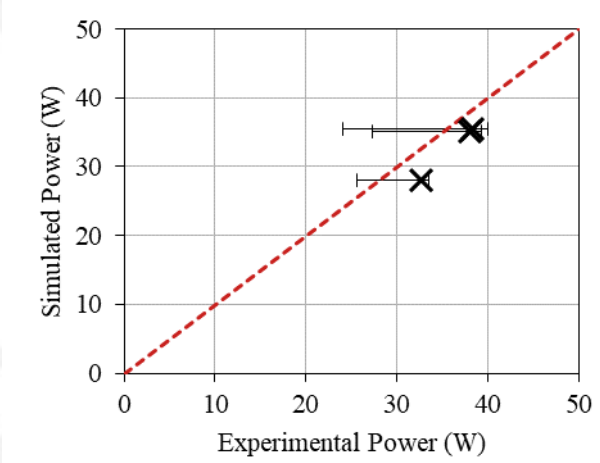

Fig. 5. model evaluation - a comparison between experimental data points and matching simulations.

It was observed that simulated power and experimental power matched within the range of experimental uncertainty for each of the data points. Therefore, the model was deemed an appropriate approximation of screw pump performance. Further, the power required by the simulated screws was less than the experimental screws, which lends further credence to the accuracy of the simulations; the simulated screw is an idealized screw that is not subjected to additional mechanical losses (like bearing losses) that were present in the laboratory screws. Therefore, the simulated screw should be expected to perform the same water lifting action with less required power.

2.4 Simulation Set

A set of 20 simulations were originally planned to test the performance of screw pumps across a range of input parameters and scale sizes. The screw's main input parameters are the upper water level, lower water level, and rotation speed. To match practical design guidelines, the lower water level was set to its numerical optimal (cf. Eqn. 3) and the upper water level was set to its practical design setting of zero. Therefore, only the rotation speed was required to vary for this dataset. Muysken and Nagel suggest that screws may range from about 15 to 60 RPM [25], [26], and that smaller screws should operate at higher speeds. So, simulations were conducted from 10 to 100 rev/min

by increments of 10 rev/min. After the dataset was gathered, and additional simulation was run at 15 rev/min to address a noticeable gap in the observed performance trends.

The operational input parameters impact on screw performance was to be investigated across two scale sizes of screws since the literature alludes to a noticeable distinction between small- and large-diameter screws. As such, simulations were design that matched the laboratory screw in size. To maintain consistency with a CFD study of Archimedes screw generators and allow for comparisons between the two systems. The authors believe there may be added value in investigating Archimedes screw performance as a whole (as a pump and in its "reverse" orientation as a generator). This may be particularly valuable when modelling gap leakage loss since a first-principles model exists for ASGs; it might be possible to modify the model's velocity term to extend its range of application to include both ASGs and ASPs. To allow for more direct comparisons between the models, the same screw geometries were used – they are shown in the table below:

Table 2. simulated screw geometries; screws are proportionally identical and designed to match dimensionally with a similar study on Archimedes screw generators for hydropower production *[34]*.

	Scale	D_o (m)	D_i (m)	S (m)	L (m)	N (-)	β (°)	G_w (m)
Screw 1	0.47	0.148	0.079	0.148	0.572	3	24.5	0.002
Screw 2	1.00	0.316	0.168	0.318	1.219	3	24.5	0.002
Screw 3	2.13	0.675	0.359	0.678	2.603	3	24.5	0.004
Screw 4	3.16	1.000	0.532	1.004	3.856	3	24.5	0.006
Screw 5	6.33	2.000	1.064	2.008	7.711	3	24.5	0.008
Screw 6	11.07	3.500	1.863	3.514	13.50	3	24.5	0.010
Screw 7	15.81	5.000	2.661	5.020	19.28	3	24.5	0.010

It is noted that Screw 2 is a dimensional match to the laboratory-scale screw used in the model evaluation. As well, all the screws in the table are linearly scaled versions of Screw 2 – in other words, they are proportionally identical to Screw 2, just larger or smaller. For this study, Screw 2 and Screw 5 were used to investigate the performance of a very small laboratory-screw and a large, real-world scale screw.

Both Screw 2 and Screw 5 were simulated across the range of rotation speeds mentioned above at their optimal lower water levels and an upper water level of 0. The goal of the simulations was to investigate how mechanical efficiency changed with rotation speed for each scale size. It was found that efficiency was impacted significantly by friction loss, so that was explored next.

Mechanical efficiency is an important factor when designing screws, but the delivered flow rate (the user-facing parameter) is often the most important. So, the dimensionless flow rate was compared against the rotation speed to determine the effectiveness of flow delivery. It was observed that dimensionless flow rate varier in the upper speed range, so a series of probes were placed along the screw's trough to measure the bucket fill height along the screw's length during operation. The results demonstrated

that the filling of the first bucket of the screw may be impacted by the rotation speed, so that relationship was investigated as well.

3 Results

First, the mechanical efficiency of the two scale-sized screw pumps were compared across the range of rotation speeds.

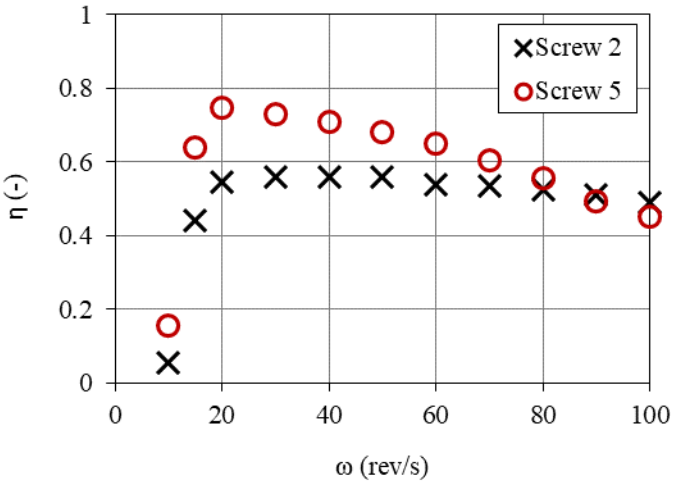

Fig. 6. mechanical efficiency across rotation speed range for Screw 2 and Screw 5.

It was observed that the different scale-sized screws had different mechanical efficiency curves, and different efficiency peaks. The smaller screw seemed to have a maximum efficiency between 30 and 50 rev/min. It retained a similar level of mechanical efficiency throughout the majority of the speed range. It was least efficient at speeds lower than 20 rev/min, or higher than 80 rev/min. To three significant digits, the highest measured efficiency in the smaller screw was observed at rotation speeds of 30 and 40 rev/min; it had a value of 56.1%. The 50 rev/min setting had an efficiency of 56.0% - it had the same efficiency to two significant digits.

The larger screw had an efficiency peak between 15 and 30 rev/min. It became much less efficient at rotation speeds of 15 rev/min and lower, and its efficiency dropped off steadily as rotation speed increased from 30 rev/min. The highest measured efficiency of the larger screw occurred at 20 rev/min in which the screw operated at 74.9% efficiency.

The efficiency values seem to correspond reasonably well with the recommendations by Muysken [26] and Nagel [25]. The larger screw is a reasonably sized screw for real-world applications, and it operated with a peak measured efficiency of about 75%, matching Muysken's maximum efficiency suggestion. Screw 2 was much smaller than

a practical, real-world screw – it was not of a size that was considered by Muysken or Nagel.

It is interesting to note the difference in efficiency between the two length scales. The larger screw generally performs with higher mechanical efficiencies, though it is much more susceptible to the effects of rotation speed. This suggests that there are dynamic effects that impact performance of larger screws more than smaller screws. As such, the frictional power loss was compared to rotation speed next (Fig. 7).

To allow for a more direct comparison, the frictional power loss was scaled by the shaft power. That allowed for a dimensionless and directly proportional comparison between the small and large screws.

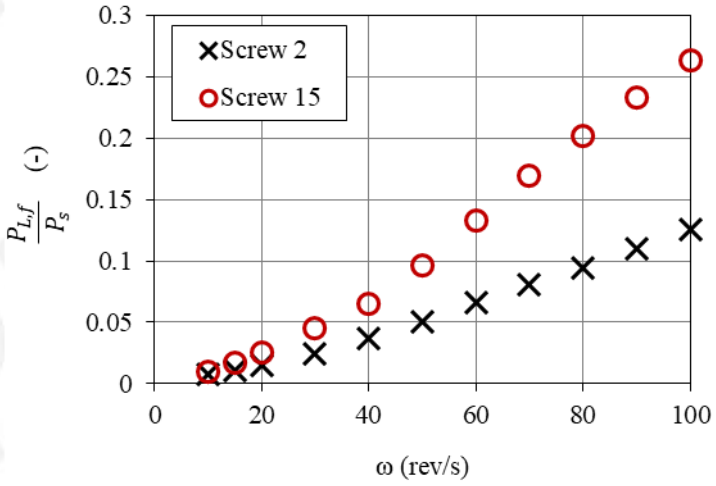

Fig. 7. dimensionless frictional power loss across rotation speed range for Screw 2 and Screw 5.

It can be observed that, in the low rotation speed range, the friction loss is the same for both the small- and large-scale screws in proportion to the shaft power. However, when the rotation speed increased, the larger screw's friction loss increased substantially and at a much higher rate than the smaller screw. That may explain why the larger screw had a steeper efficiency drop off in Fig. 6 when compared to the smaller screw. The larger screw had a larger surface area, and much higher tangential velocities near its blade tips that contributed to its proportional increase in frictional power loss.

The flow rate was then compared across the range of rotation speeds for each screw. Again, to allow for a direct comparison, a dimensionless term was used; the flow rate was divided by the product of the transport velocity and the outer diameter squared.

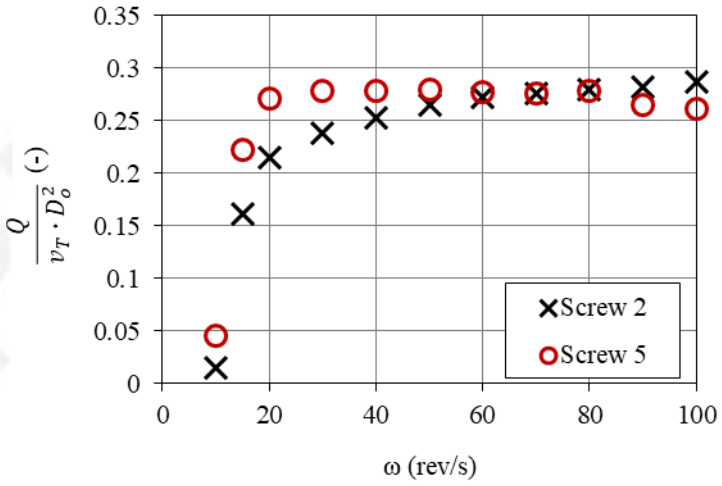

Fig. 8. dimensionless flow rate across rotation speed range for Screw 2 and Screw 5.

The comparison demonstrated that the larger screw was more effective at volumetric transport in the low rotation speed range. That was likely because Screw 5 was much larger by volume, and its blade-trough gap was proportionally much smaller. Therefore, there was proportionally much less gap leakage during operation in the large screw compared to the small screw. As such, the larger screw was able to operate more efficiently at a lower rotation speed, and the small screw could not discharge as much volumetric flow rate since it was effected by gap leakage at a proportionally much higher rate.

Conversely, at high rotation speeds the larger screw had a drop-off in dimensionless flow rate. During operation, it was observed that the larger screw was not able to fill its bucket's optimally since its blades were not open to the lower basin for a sufficient time during water in-rush at the inlet. That was not a significant problem in the smaller screw; it seemed that the smaller screw was able to fill its much smaller bucket volume throughout the entire rotation speed range. It seemed that the larger screw's inlet had a proportionally more impactful flow constriction than the small screw. Neither screw seemed to perform with substantial dimensionless flow rates at lower rotation speeds – effectively, the screws were both barely overcoming the gap leakage flow rate during low-speed operation (i.e., 10 rev/min).

The effective flow rate drop-off of the large screw was of particular interest. To investigate the cause of that further, more post-processing of the data was required.

It was observed during experimentation and recent site visits that the water level in the screw's buckets varied along the length of the screw's trough during operation. It was particularly noticeable in longer screws. It is postulated that this was due to gap leakage in the screw. In screw pumps, gap leakage is cumulative during conveyance; as the bucket translates along the length of the screw, its leakage through the gap compounds. So, if rotation speed is held consistent, a longer screw would deliver less flow

rate at its output, and its top bucket would have a much lower water level than its bottom bucket.

To investigate this phenomenon, probes were set along the length of the simulated screw's trough to measure water levels in the screw's buckets throughout the simulation. Five probes were used – they were equally spaced along the length of the screw's trough, as shown in Fig. 9.

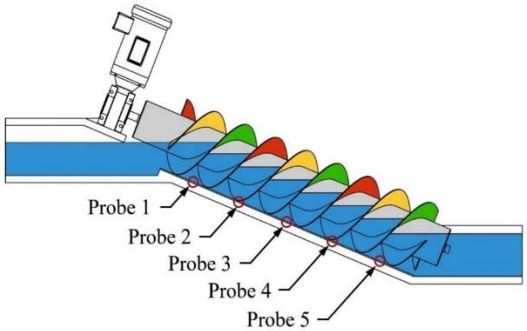

Fig. 9. bucket fill height probe locations in simulated domain.

A post-processing script was generated to calculate the time-averaged, dimensionless bucket fill height ratio above each probe. The results were then compared to rotation speed. To aide in visualization, the fill height was plotted against a dimensionless distance along the screw's trough – it was non-dimensionalised by the length of the screw and normalized by the pitch length. Effectively, the x-axis displays the dimensionless length along the trough in units of dimensionless pitch lengths (or revolutions of the helix). It is noted that Screw 2 and Screw 5 have length ratios of $\lambda = L/s = 3.84$. To prevent clutter on the plots, 6 curves were presented that vary by rotation speed; allowing for direct comparisons of the bucket filling patterns along the trough for different rotation speeds.

After the 5 probes were plotted, two additional points were added to represent the fill height corresponding to the lower basin water level (at $x \cdot L/S = 0$) and the upper basin water level (at $x \cdot L/S = 3.84$).

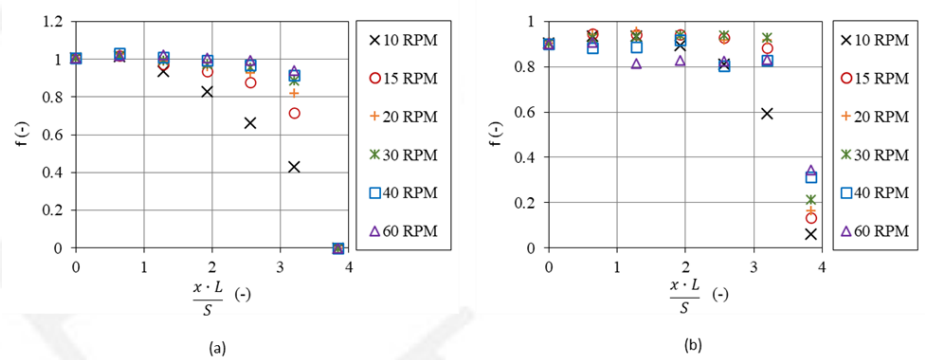

Fig. 10. bucket fill height ratio along screw trough for Screw 2 (a) and Screw 5 (b).

It was observed that, for low and moderate rotation speeds, the first bucket had a similar fill height to the lower basin water level setting. Generally, the fill height of the buckets decreased as water translated up the screw. As mentioned, it was mostly due to the cumulative effects of gap leakage during conveyance. This seemed evident based on the plots – the gap leakage is mainly driven by hydrostatic pressure, so as rotation speed increased, the bucket spent less time in conveyance experiencing gap leakage. In slower-speed screws, the buckets have more time to leak during conveyance, so the difference in water levels was more extreme as evidenced by the 10 rev/min curve.

As the rotation speed increased past 60 rev/min in Screw 2, and 30 rev/min in Screw 5, the buckets became much more dynamic and exhibited much less predictable trends on these plots – that was another reason that only 6 curves were presented for Screw 2 and Screw 5. The curves for 40 and 60 rev/min in Screw 5 show the less predictable trends which indicate dynamic effects not present in lower-speed operation. However, it seemed valuable to show how the rotation speed impacted the filling of the first screw bucket, so the bottom-most probe (i.e., at $x \cdot L/S = 0.640$) was plotted against the entire rotation speed range for Screw 2 and Screw 5. The following plot also added additional evidence to the ideas presented in the discussion of Fig. 8.

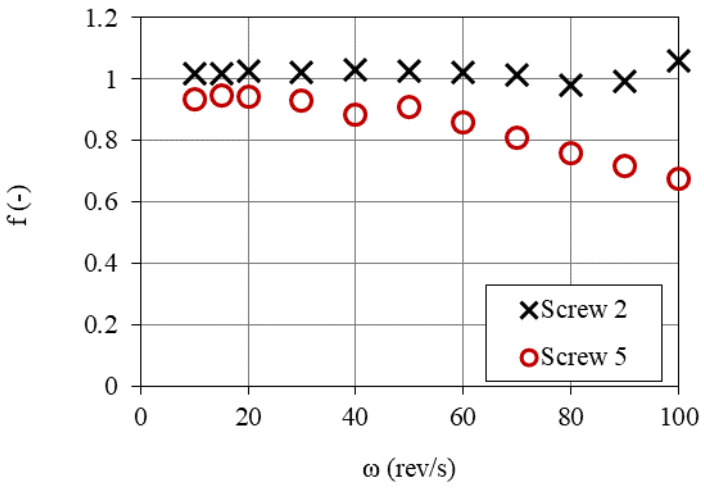

Fig. 11. bucket fill height of the first fully-enclosed screw bucket (i.e., corresponding to Probe 5 in Figure 8)

Screw 2 and Screw 5 were both set to operate at their optimal lower water levels; this setting should correspond to an initial bucket fill height of $f = 1$. Screw 5 seemed to operate with a lower water level that was slightly under its optimal point, so it should perform with bucket fill height ratios near approximately $f = 0.94$.

It was observed that Screw 2 was able to fill its 1st bucket at or above its designed level of $f = 1$ for the entire rotation speed range. Since Screw 2 was a laboratory-scale screw, it had proportionally very low bucket volume when compared to Screw 5. Within the tested rotation speed range, Screw 2 was able to fill its bottom buckets without an observable hinderance or flow constriction.

Conversely, it was observed the Screw 5's first bucket was only able to optimally fill at rotation speeds below 30 rev/min. At 30 rev/min and above, the water level in the first bucket was less than the available water level in the lower basin – indicating that it had not completed filling. The large difference in scale size between Screw 2 and Screw 5 may have led to a change in flow regime which impacted the ability of water to in-rush between the first bucket's blade openings at the inlet of the screw during operation at higher rotation speeds.

These observations also seemed to reinforce some of the empirical guidance given by Muysken and Nagel. Using Muysken's models [26], Screw 5 should be operating at a rotation speed of 31.5 rev/min, which, though it is not optimal, is in a range of operation that corresponds to good first-bucket filling (Fig. 11), low impacts of gap leakage loss (Fig. 10), highly effective dimensionless flow conveyance (Fig. 8), lower frictional power loss effects (Fig. 7), and high efficiency (Fig. 6). Though the empirically-driven guidelines seemed to perform reasonably well, they are not optimal, and there is much room for improvement.

4 Conclusion

A novel computational fluid dynamic model of Archimedes screw pumps was developed in this study. The model was tested for sensitivity of its mesh resolution to find a balance between accuracy and computational efficiency. It was then compared to experimental laboratory data to evaluate its accuracy; it was suggested that the CFD model was an accurate approximation of Archimedes screw pump performance.

The CFD model was then used to gather a wide range of performance data to introduce much-needed data and analysis to the literature to aide in future model development and improvements. Data was gathered from two scale-sized screws to investigate the performance impacts of rotation speed for small and large screw pumps.

It was observed that the larger screw operated with a higher peak mechanical efficiency, but was proportionally more impacted by friction loss in the high-speed range. The larger screw's buckets filled less during high-speed operation, leading to an underfilled screw that is proportionally more impacted by friction effects, and operates with much lower efficiencies.

It was shown that the optimal efficiency of Screw 5 (Do = 2 m) was near 20 rev/min, though current empirical-models suggest it should be set to a rotation speed of about 31.5 rev/min. It was shown that Screw 2 (Do = 0.316 m) operated at its maximum efficiency between 30 and 50 rev/min; current models suggest that Screw 2 should operate at a rotation speed of about 108 rev/min.

It was also observed that gap leakage had a cumulative effect on the screw during conveyance such that lower-speed operation had a significant change in bucket fill height along the length of the screw.

Altogether, the novel CFD model, data, and analysis presented in this study should be a substantial aide to future research in screw pump characterization, design, and optimization.

Acknowledgements

Aspects of this work were financially supported by the Natural Sciences and Engineering Research Council (NSERC) of Canada's Alliance program (grant ALLRP 561188-20) and Greenbug Energy Inc. (Delhi, ON, Canada). The assistance of Tony Bouk and Brian Weber of Greenbug Energy Inc. is gratefully acknowledged. The authors would also like to acknowledge the assistance of Amir A. Aliabadi (University of Guelph), Leo Guiot de la Rochere (ENGEES), and Leandro Duarte (ENGEES).

References

[1] C. Rorres, "The Turn of the Screw: Optimal Design of and Archimedes Screw," *J. Hydraul. Eng.*, vol. 126, no. 1, pp. 72–80, 2000.

[2] S. Dalley and J. P. Oleson, "Sennacherib, Archimedes, and the Water Screw: The Context of Invention in the Ancient The Context of Invention in the Ancient World,"

Technol. Cult., vol. 44, no. 1, pp. 1–26, 2003.

[3] T. Koetsier and H. Blauwendraat, "the Archimedean Screw-Pump : a Note on Its Invention and the Development of the Theory," *Proc. Int. Symp. Hist. Mach. Mech. (HMM04). Kluwer, Dordercht*, pp. 181–194, 2004.

[4] A. I. Wilson, "Classical water technology in the early Islamic world," *Institutum Rom. Finlandiae*, no. January 2003, pp. 115–411, 2003.

[5] Ḥarīrī and Y. ibn M. Wāsiṭī, *Maqamat Al-Hariri*. London: Bibliothèque nationale de France, 2003.

[6] I. Bobbink, "De Landschapsarchitectuur van het Polder-boezemsysteem," Sirene Ontwerpers, Rotterdam, 2016.

[7] L. White Jr., *Medieval technology and social change*. London: Oxford University Press, 1974.

[8] G. Nagel and K.-A. Radlik, *Wasserförderschnecken: Planung, Bau und Betrieb von Wasserhebeanlagen*, 1e ed. Berlin: Pfriemer Buchverlag in der Bauverlag, 1988.

[9] Karl-August Radlik, "Hydrodynamic screw for energy conversion - uses changes in water supply to regulate energy output," DE4139134A1, 28-Nov-1991.

[10] H. Addison, "Experiments on an Archimedean screw," *Inst. Civ. Eng.*, no. 75, 1929.

[11] A. Poosti and F. M. Lewis, "Pump replacement at the Hyperion Intermediate Pump Station: Analysis of Archimedes Screw vs Vertical Turbine Pumps," Los Angeles, 2002.

[12] E. A. Asli-Ardeh and A. Mohsenimanesh, "Determination of effective factors on power requirement and conveying capacity of a screw conveyor under three paddy grain varieties," *Sci. World J.*, vol. 12, no. 1, 2012.

[13] S. S. Waje, B. N. Thorat, and A. S. Mujumdar, "Hydrodynamic Characteristics of a Pilot-Scale Screw Conveyor Dryer," *Dry. Technol.*, vol. 25, pp. 609–616, 2007.

[14] FishFlow Innovations, "Fish Friendly Screw Pump: Pump as Fish Passage," *fishflowinnovations.nl*, 2019. [Online]. Available: http://fishflowinnovations.nl/en/innovations/screwpump/#1483537045652-5ec9b0e6-032c. [Accessed: 03-Dec-2020].

[15] M. G. Mesa, L. P. Gee, L. K. Weiland, and H. E. Christiansen, "Physiological Responses of Adult Rainbow Trout Experimentally Released through a Unique Fish Conveyance Device," *North Am. J. Fish. Manag.*, vol. 33, pp. 1179–1183, 2013.

[16] E. D. Weber and S. M. Borthwick, "Plasma Cortisol Stress Response of Juvenile Chinook Salmon to Passage through Archimedes Lifts and a Hidrostal Pump," *North Am. J. Fish. Manag.*, vol. 22, pp. 563–570, 2002.

[17] A. Strizhak, U. Vakhidov, A. Lipin, R. Dorofeev, A. V Sogin, and L. S. Mazunova, "Modelling of vehicles with rotary-screw propulsion unit along water- flooded substructure Modelling of vehicles with rotary-screw propulsion unit along water-flooded substructure," in *Journal of Physics: Conference Series*, 2019.

[18] M. DiFrangia, "The hydraulics of injection molders," *FluidPower World*, Cleveland, May-2016.

[19] L. B. Kreuziger and M. P. Massicotte, "Adult and pediatric mechanical circulation : a guide for the hematologist," *Hematology*, vol. 2018, no. 1, pp. 507–515, 2018.

[20] S. R. Waters and G. A. Aggidis, "Over 2000 years in review: Revival of the Archimedes Screw from Pump to Turbine," *Renew. Sustain. Energy Rev.*, vol. 51, pp. 497–505, 2015.

[21] J. Monserrat, R. G. Ortiz, L. Cots, and J. Barragán, "Energy Saving in a Variable-

Inclination Archimedes Screw," *Irrig. Drain. Syst. Eng.*, vol. 04, no. 01, 2015.

[22] M. Lyons, S. Simmons, M. Fisher, J. S. Williams, and W. D. Lubitz, "Experimental Investigation of Archimedes Screw Pump," *J. Hydraul. Eng.*, vol. 146, no. 8, pp. 1–10, 2020.

[23] R. J. Hoeksema, *Designed for Dry Feet: Flood Pretection and Land Reclamation in the Netherlands*, 1st ed. Reston: American Society of Civil Engineers, 2006.

[24] F. Hassan, "Water history for our times," *IHP essays water Hist.*, vol. Vol. 2, 2011.

[25] G. Nagel, *Archimedian Screw Pump Handbook: Fundamental Aspects of the Design and Operation of Water Pumping Installations Using Archimedian Screw Pumps*, 1st ed. Schwäbisch Gmünd: RITZ-Pumpenfabrik OHG, 1968.

[26] J. Muysken, "Berekening van het nuttig effect van de vijzel," *Ing.*, vol. 21, pp. 77–91, 1932.

[27] Storm and Buyzing, "Werktuig un Scheepsbow Modellversuche an Wasserförderschnecken (Model tests on Archimedian screw pumps)," 1851.

[28] I. G. Horch, "Die Wasserförderschnecken (The Archimedean screw pump)," *Ing.*, p. 945 et seq., 1916.

[29] Bekkering, "Fliessgeschweindigkeiten un Drehzahlen an Wasserförderschnecken (Rates of flow and speeds of Archimedian screw pumps)."

[30] G. Nagel, "Die Wasserförderschnecken als Vorflut- und Abwasserpumpe," *GWF*, vol. 52, 1959.

[31] Hütte, *Drehzahlen an Schneckenförderern*. Berlin: Springer-Verlag.

[32] D. M. Nuernbergk, *Wasserkraftschnecken - Berechnung und optimaler Entwurf von archimedischen Schnecken als Wasserkraftmaschine (Hydropower screws - Calculation and Design of Archimedes Screws used in Hydropower)*, 2nd ed. Detmold: Verlag Moritz Schäfer, 2020.

[33] S. C. Simmons, L. Miller, and W. D. Lubitz, "Review and evaluation of Archimedes screw pump design guidance," in *Responsible Engineering and Living*, D. S.-K. Ting and A. Vasel-Be-Hagh, Eds. Basel: Springer Nature, 2022.

[34] S. C. Simmons, "An experimental and numerical analysis of parameter scaling in Archimedes screw generators by," University of Guelph, 2021.

[35] J. Wijdieks and M. G. Bos, "Pumps and Pumping Stations," in *Drainage principles and applications*, H. P. Ritzema, Ed. Wageningen: International Institute for Land Reclamation and Improvement, 1994, pp. 965–999.

[36] A. Lashofer, W. Hawle, and B. Pelikan, "State of technology and design guidelines for the Archimedes screw turbine," in *Hydro 2012 - Innovative Approaches to Global Challenges*, 2012, no. October, pp. 1–8.

[37] A. Kozyn, S. Ash, and W. D. Lubitz, "Assessment of Archimedes Screw Power Generation Potential in Ontario," in *4th Climate Change Technology Conference*, 2015, no. 4, pp. 1–11.

[38] M. Lyons and W. D. Lubitz, "Archimedes screws for microhydro power generation," in *Proceedings of the ASME 2013 7th International Conference on Energy Sustainability & 11th Fuel Cell Science*, 2013, pp. 1–7.

[39] F. R. Menter, "Two-equation eddy-viscosity turbulence models for engineering applications," *AIAA J.*, vol. 32, no. 8, pp. 1598–1605, 1994.